Indian Journal of Chemistry
Vol. 57A, January 2018, pp. 26-33

In situ synthesis and characterization of Prussian blue nanocubes on graphene oxide and its application for H_2O_2 reduction

Cheng-xiang Ge[a], Peng-jun Li[b], Juan-hua Lai[c] & Ping Qiu[b,*]

[a]Hefei Center for Disease Control and Prevention of Anhui Province, Hefei 230061, China

[b]Department of Chemistry, Nanchang University, Nanchang 330031, China

Email: pingqiu@ncu.edu.cn

[c]Jiangxi Medical Device Testing Center, Nanchang 330047, China

An effective and facile in situ electroless deposition approach has been developed for growing high-quality Prussian blue nanocubes on the surface of graphene oxide (PBNCs/GO) in a controlled manner. The resulting hybrids are characterized by scanning electron microscopy, transmission electron microscopy, Fourier transform infrared, ultraviolet visible, X-ray diffraction and electrochemical techniques. The electrochemical behavior on the modified electrode is discussed in detail. A linear calibration of the biosensor is obtained in the range of 0.002–2.8 mM with a detection limit of 0.48 μM. The response is within less than 5 s and the detection sensitivity is 2502 μA $mM^{-1}cm^{-2}$. The proposed approach allows simple and controlled preparation of transition metal hexacyanoferrate nanocrystals/graphene oxide and is promising for the study of unique shape-, size-, and structure- dependent properties for optoelectronic, magnetic, and electrocatalytic applications.

Keywords: Nanocubes, Prussian blue nanocubes, Graphene oxide, Reduction, Hydrogen peroxide reduction, Biosensors

Prussian blue (PB) is a prototype of metal hexacyanoferrates with well-known electrochromic[1, 2], electrochemical[3], photophysical[4], and magnetic properties[5] and potential analytical applications[6]. Since it strongly catalyzes the reduction of hydrogen peroxide at low operating potentials[6], PB is denoted as an "artificial enzyme peroxidase" and has been extensively used in the construction of electrochemical biosensors. The main drawback of PB as an electrocatalyst in respect to long-term continuous monitoring is the inherent instability, particularly in neutral solutions. Firstly, the PB layer is mechanically unstable. Secondly, the long-term operational stability is affected by the product of hydrogen peroxide reduction at PB modified electrodes, known to be the hydroxyl ion (OH^-)[7]. Moreover, various iron complexing agents (for instance, EDTA used as blood anticoagulant) are known to solubilize ferric hexacyanoferrate. To solve the problem, high-quality active supports are usually required for the immobilization of PB. Thus, much endeavor has been devoted to fabricating new supports that can improve the sensor's stability and activity[8-10]. Among these investigated support materials, CNTs have been a focus of research because of their unique stability and ion-loading capacity. Nevertheless, when constructing PB/CNTs composites electrochemical sensors, multistep processes are usually required to prepare and purify CNTs or to presynthesize PB nanoparticles[8, 9], which limited their applications to a large extent.

The recent emergence of graphene nanosheets has opened a new avenue for utilizing new 2D carbon material as a support because of its high conductivity (10^3-10^4 S/m), huge surface area (calculated value, 2630 m^2/g), unique graphitized basal plane structure, and potential low manufacturing cost[11,12]. Herein, graphene oxide (GO) is one of the most crucial derivatives of graphene nanosheets and a large number of studies have described the dispersion and exfoliation of GO [13,14]. This material chemically functionalized with oxygen groups such as hydroxyls and epoxides can stabilize the dispersion of the nanosheets in water[15]. From the chemical point of view, the presence of oxygen functionalities at GO surface may be very interesting because they provide reactive sites for chemical modification by deposition of known carbon surface chemistry materials[16]. In the case of PB nanoparticles deposited on CNTs for example, CNTs are often introduced by strong sulfuric/nitric acid treatment[8,9]. In contrast, GO nanosheets are directly obtained from the chemical exfoliation of graphite, which indicate that the essential oxygen chemical functionalities for further chemical reactions are already present. This feature, together with the high

specific surface area of GO, makes them promising materials for catalytic applications[17,18]. To date, a number of examples of graphene/PB composite have been reported. Direct electrode position of PB on graphene matrix is a traditional method[19]. However, direct electrodeposition is always difficult and the PB films obtained are also loose, which result in poor adhesion and limited specific surface area. The other recently emerged method to form PB on graphene is to reduce Fe^{3+} using polyethyleneimine (PEI) as reductant[20] or grow PB on functional graphene[21]. However, all these methods require addition of extra reagents, which seems somewhat complicated and also the conductivity of graphene could be reduced. Recently, a green synthesis method of graphene/PB composite has been also reported[22]. However, in this study, it takes a long time that the PB grows on the graphene.

In this study, we demonstrate an *in situ* electroless deposition approach for the synthesis of GO-supported PB nanocubes (PBNCs/GO) composite nanomaterials and tried preliminarily to apply it to the fabrication of the sensors. The method using GO as support has several important advantages: (a) The nanocomposites could be produced directly from GO in an *in situ* wet-chemical reaction, where the GO acts as both reductant and template/stabilizer. (b) The size and morphology of PB on the surface of GO could be easily controlled by simply changing the synthetic parameters, such as the initial molar concentration of $FeCl_3$ and $K_3[Fe(CN)_6]$, the temperature, duration of the heat treatment and the pH value. We have studied the electrochemical sensing of hydrogen peroxide with the PBNCs/GO composite film modified the electrode (Fig. 1) and found that PBNCs/GO nanocomposite exhibited prominent electrocatalytic activity towards the reduction of hydrogen peroxide, which can be explained by the remarkable synergistic effect of the GO and PB. This novel method is expected to be applicable for preparation of other coordination polymer/GO composite and applications for electronic nanodevices.

Materials and Methods

Graphite flake (99.8%, 325 mesh) was purchased from Alfa Aesar Company. All other reagents were commercially available and of analytical grade. All solutions were prepared using doubly distilled water.

Scanning electron microscopy (SEM) images were obtained by using a Quanta 200 scanning electron microscope (FEI, USA). Transmission electron microscopy (TEM) images were obtained on a JEM-2010 transmission electron microscope (JEOL Ltd.). The Fourier-transform infrared (FTIR) spectra of samples in KBr pellets were recorded on a Nicolet 5700 FTIR spectrometer (Nicolet, USA). UV-vis absorption spectra were recorded with a UV-2450 spectrophotometer (Shimadzu). X-ray diffraction (XRD) patterns of the nanocomposites were obtained using a Rigaku powder diffractometer equipped with Cu-Kα_1 radiation (λ = 1.5406 Å). Electrochemical experiments were carried out on a PGSTAT30/FRA2 system (Autolab, The Netherlands). A three-electrode system was used with a saturated calomel electrode (SCE) as the reference electrode, a platinum wire as the auxiliary electrode, and the modified AuE as the working electrode.

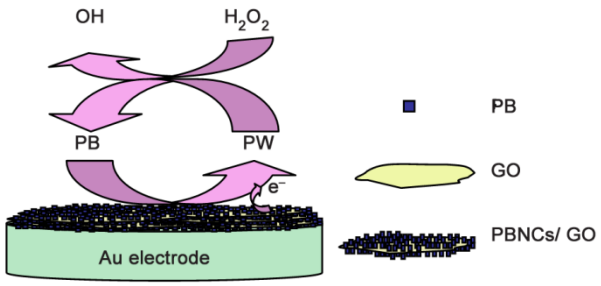

Fig. 1 — Schematic representation of PBNCs/GO/Au nanocomposite and the electrocatalytic mechanism for H_2O_2 reduction.

Preparation of graphene oxide

The GO was obtained from graphite flake by Hummers' method [23]. Firstly, 0.5 g of graphite, 0.5 g of $NaNO_3$, and 23 mL of H_2SO_4 were stirred together in an ice bath and 3 g of $KMnO_4$ was gradually added under stirring. The mixture was kept below 20 °C. Successively, the solution is transferred to a 35±5 uc water bath and stirred for about 1 h, forming a thick paste, followed by the addition of 40 mL of ultrapure water. After the temperature was increased to 90±5 °C, the mixture was stirred for 0.5 h. Finally, 100 mL of ultrapure water was added, followed by the slow addition of 3 mL of H_2O_2 (30%). The color of the mixture changed from dark brown to yellow and no gas was being produced. The warm solution was then filtered and washed three times with 5% aqueous HCl to remove metal ions and then washed with ultrapure water to remove the acid. The filter cake was dispersed in ultrapure water. The obtained brown dispersion was then subjected to 5 min of centrifugation at 3000 rpm to remove any unexfoliated graphite oxide. Exfoliation was obtained after 2 h of ultrasonic treatment.

Preparation of Prussian blue nanocubes/graphene oxide composite

To prepare the Prussian blue nanocubes/graphene oxide composite, 10 mL of GO (10 mg/mL) was dispersed in 90 mL water ultrasonication. Seven samples (1–7) were prepared by the following procedure: first, 5 mL as-prepared GO solution was placed in a round bottom flask, then 0.2 mL of the two-component aqueous solution, $FeCl_3$+$K_3[Fe(CN)_6]$ (equimolar amount, pH 1.6), with initial molar concentrations of 0.5, 1, 2, 5, 10, 20, 50 mM (corresponding to samples 1–7, respectively) was added. After the mixture was thoroughly mixed by vigorous stirring at 30 °C for 2 h, the color gradually changed from yellow brown to dark cyan, suggesting the formation of PBNCs/GO heterostructure. The obtained suspension was centrifuged and washed with water till the supernatants were colorless, and the final PBNCs/GO composite was then dispersed in 5 mL water for further characterization. The temperature of the mixed solution was controlled by water bath. For comparison, bulk PB was also prepared using the same procedure except that $FeCl_3$ was changed to $FeCl_2$ and without GO.

Electrode preparation and modification

The gold electrode (AuE, 2 mm dia.) was carefully polished with 1.0, 0.3, and 0.05 μm alumina slurry, and rinsed thoroughly with doubly distilled water between each polishing step. The electrode was ultrasonically cleaned with 1:1 nitric acid, ethanol, and doubly distilled water, and then allowed to dry under N_2. Finally, the clean Au electrode was coated by casting a suspension (6 μL) of the PBNCs/GO composite in water and was dried in air for more than 12 h.

Results and Discussion

For the fabrication of PBNCs/GO composite, the GO nanosheets were prepared by oxidizing graphite flake according to a modified Hummer's method[23]. As shown in Fig. 2a, single sheets of oxidizing graphite of a broad size distribution over 0.5–2 μm was observed. For more detailed structural information, TEM image of a single graphene sheet was collected. It appeared as translucent GO sheets with wrinkles and folds as shown in Fig 2b. The GO nanosheets were used as reductant and template to grow PB nanocubes for producing PBNCs/GO nanocomposite via an *in situ* reduction process. The morphology of the as-prepared PBNCs/GO composite was investigated by SEM and TEM. It was observed that well-separated nanocrystals with a size ranging from 25–30 nm spread out on or below the surface of GO nanosheets (Fig 2c, d). It is interesting that there was no PBNCs in other regions expect for GO. Dai and his coworkers[24] had observed formation of Au and Pt nanoparticles on single-walled

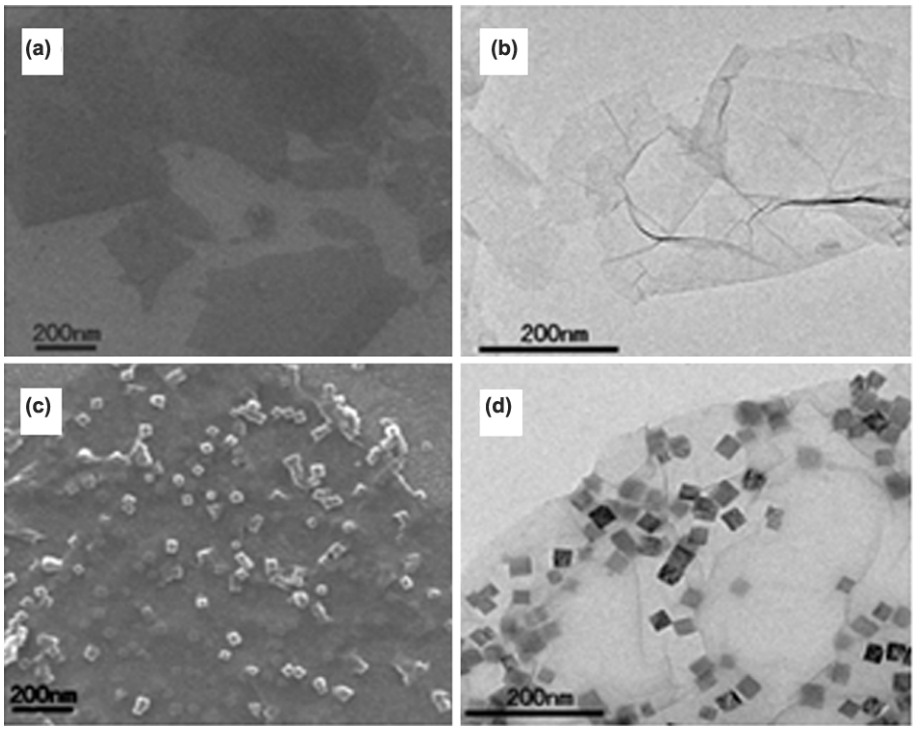

Fig. 2 — (a & c) SEM images of GO and PBNCs/GO composite. (b & d) TEM images of GO and PBNCs/GO composite.

carbon nanotubes due to spontaneous reduction of metal ions in solutions. In our previous work, the ferric ions in solution were catalytically reduced by MWNTs[9]. We found that the ferric ions in solution could also be catalytically reduced by GO. It may be assumed the Fermi level of GO is about +0.5 V above the potential of a standard hydrogen electrode (SHE), which is similar to that of single-walled carbon nanotubes[25], while the redox potential of Fe^{3+}/Fe^{2+} couple or $Fe(CN)_6^{3-/4-}$ couple are +0.77 V and +0.36 V versus SHE, respectively. It may be concluded that the relative potential levels rationalize the spontaneous electron transfer from the GO (oxidation) to the ferric ions[24], and then the reduced Fe^{2+} reacts with $Fe(CN)_6^{3-}$ to form PB immediately [9]. Similar results were obtained in the dark, under room light, halogen lamp and UV light, suggesting no significant effect of light on the electroless deposition process. This process differs from typical electroless deposition that requires reducing agents or catalyst[20], while herein it is direct redox reactions between ions and GO.

The UV-vis absorptions of GO (Fig. 3, curve 1), PBNCs/GO (curve 2) and bulk PB (curve 3), in aqueous solutions are shown in Fig. 3. The absorption peak at 230 nm was ascribed to the pure GO. On formation of the PBNCs/GO hybrid, the UV-vis absorption peak of the GO dispersion at 230 nm disappeared, which indicates that GO may be further oxidized and can be attributed to the change of the interfacial electron density at GO surface in the course of the catalytic reduction of ferric ion to ferrous ion. In addition, the broad bands with maxima at 760 nm and 720 nm for PBNCs/GO and bulk PB were observed, which is consistent with an internal charge-transfer (CT) band from Fe^{2+} to Fe^{3+} in PB[26]. Two other bands at 220 nm and 416 nm corresponding to the absorption bands of remnant potassium ferricyanide $K_3[Fe(CN)_6]$ were also observed, which may be due to incomplete washing.

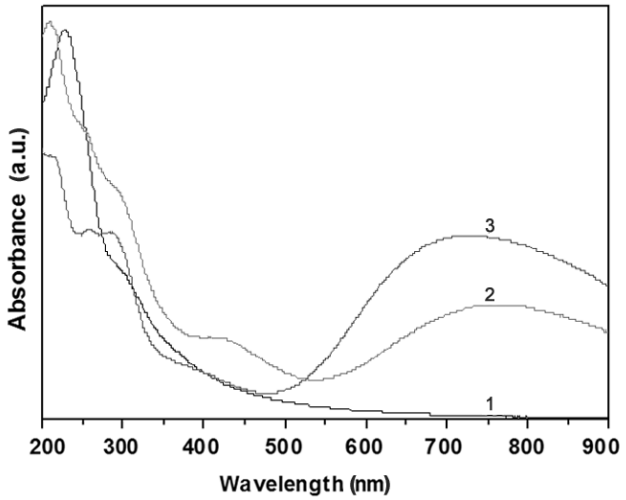

Fig. 3 — UV-vis absorption spectra of GO (curve 1), PBNCs/GO composite (curve 2), and, bulk PB in water (curve 3).

The purified GO and the PBNCs/GO composite were both analyzed using FTIR reflections after careful washing and drying. Typical FTIR spectrum of the purified GO showed absorption band at 1731cm^{-1} due to the C=O stretching (Fig. 4). The spectrum of GO also exhibited the presence of O-H ($-\nu_{O-H}$ at 3408 and 1398 cm^{-1}), C=C ($\nu_{C=C}$ at 1624 cm^{-1}), and C-O (ν_{C-O} at 1055 cm^{-1})[27,28]. Compared with the purified GO, three new peaks of PBNCs/GO composite appeared at 2080, 602 and 498 cm^{-1}, respectively. The major band at 2080 cm^{-1} showed the usual characteristic of PB and its analogues corresponding to the stretching vibration of the CN group, while the peaks around 602 and 498 cm^{-1} can be assigned to the structure of Fe-CN-Fe[9], providing evidence for the formation of PB on GO.

The XRD patterns of the GO and the PBNCs/GO composite were collected (Fig. 5). After the formation of PB nanoparticles on the surface of GO, new diffraction peaks at 2θ(°): 17.40, 24.70, 35.23, 39.54, 50.02, 54.06, and 57.31 were assigned to the (200), (220), (400), (420), (440), (600), and (620) reflections of the PB, respectively [9]. The XRD results further indicate that PB nanoparticles were newly introduced on surfaces of GO, thus supporting the SEM and TEM images, and IR and UV–vis spectra.

Molar ratio of $K_3Fe(CN)_6$/GO

To investigate the influence of coverage and size of PB nanoparticles on GO surface, a series of control

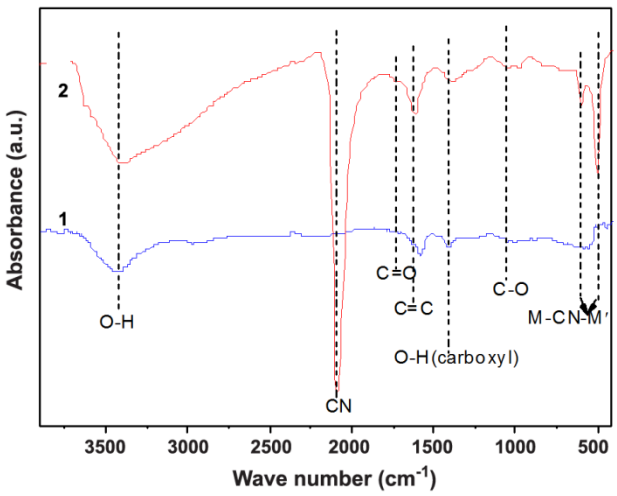

Fig. 4 — FT-IR spectra of GO (1) and PBNCs/GO composite (2).

experiments were performed. Samples (1–7) with corresponding initial molar concentrations of 0.5, 1, 2, 5, 10, 20, 50 mM of the two-component aqueous $FeCl_3$ + $K_3[Fe(CN)_6]$ (1.0 mg/mL GO) were prepared to examine the influence of initial molar concentrations of the two-component solution on morphology of the composite. Figure 6 shows typical SEM images of samples 2, 3, 4, and 7. With the initial molar concentration of 2 mM of aqueous [$FeCl_3$+$K_3[Fe(CN)_6]$] solution, a small quantity of PB NPs was decorated on GO (Fig. 6a). The PB NPs with average diameter of 12.2 nm dispersedly adhered to the GO surface, with little aggregation of PB NPs. The packing density of the attached PB NPs increased gradually with the increase in initial molar concentration of the two-component system (Fig. 6(a-d)). At the molar concentrations of 5 mM, the loading of NPs on GO increased markedly (Fig. 6b). The PB NPs with average diameter of 22 nm were not well-defined in shape, and included round and cube shapes. At the molar concentrations of 10 mM, the PB NPs turned into perfect cubic crystals with average diameter of 27 nm. Interestingly, at the molar concentration of 50 mM, it was noted that the loading of PB nanoparticles and the packing density on GO further increased (Fig. 6d). The close-packed PB NPs on GO formed aggregates and were likely to further form heterogeneous nanowires.

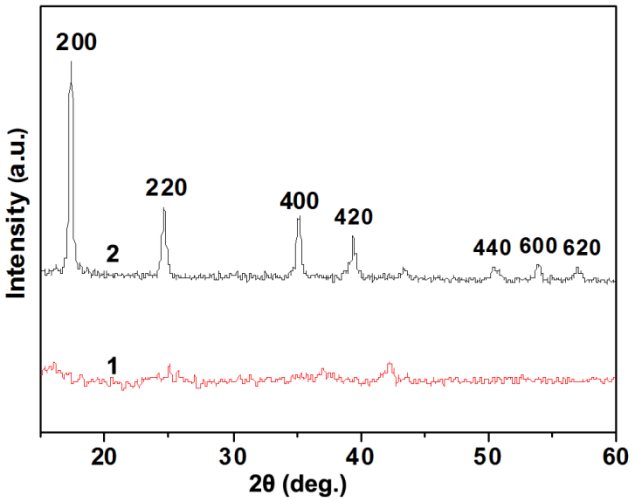

Fig. 5 — XRD patterns of GO (1) and PBNCs/GO composite (2).

Effects of reaction temperature, time and pH

The influence of reaction temperature on the morphology of the PBNCs/GO composite was studied. With increasing the reaction temperature, the average size, shape and density of the PB NPs on the surface of GO were affected significantly. When the mixed solutions were cooled at 0 °C for 120 min, a small number of irregular PB NPs with size of ~28 nm were found not only on the surface of GO sheets, but also

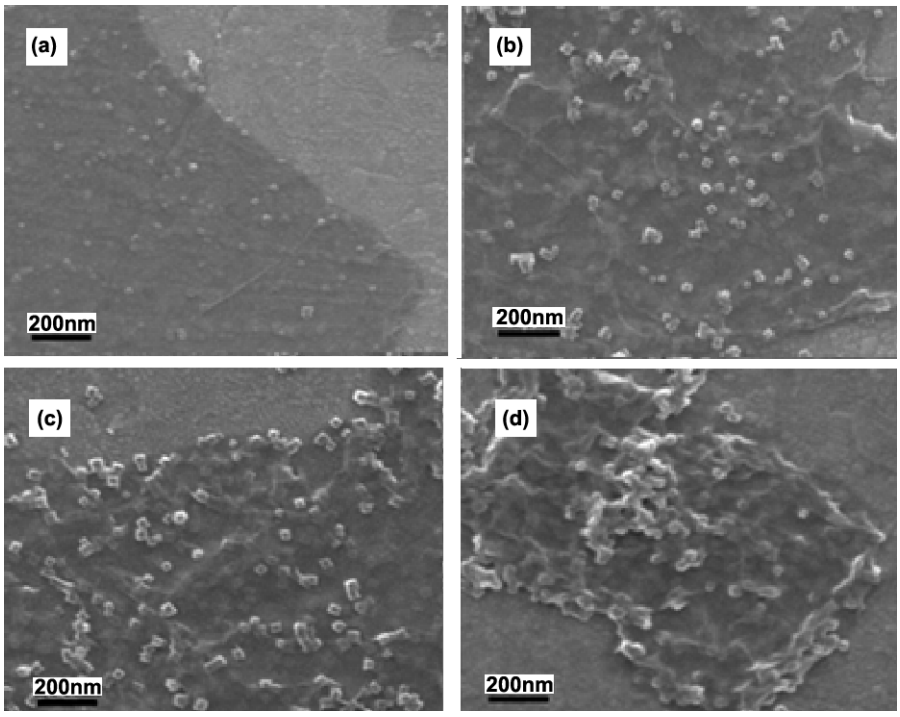

Fig. 6 — SEM images of PBNCs/GO composite synthesized at initial molar concentration of two-component ($FeCl_3$+$K_3[Fe(CN)_6]$)[2]. [(a) 2 mM; (b) 5 mM; (c) 10 mM; (d) 50 mM].

outside the GO sheets, When the reaction temperature was increased to 30 °C, the average size of PB NCs gradually grew to 37 nm and the coverage of PB NCs increased significantly. Also, it was interesting that the PB NPs grow only on the GO surface and the PB NPs were well-defined in shape. When the reaction temperature continued to increase to 60 °C, the shape of PB NCs on the surface of GO became more perfect than that produced at a lower temperature of precursors. At the same time, the average size of PB NCs markedly increased up to 61 nm. With increasing reaction time, not only the coverage of PB NCs increased, but also the shape of PB NCs on the GO nanosheets became more regular.

The influence of reaction pH on the morphology of the PBNCs/GO nanocomposite was investigated at pH between 1.6 and 5.0. At pH 1.6, perfectly shaped cubic crystals of PB NPs and size of ~27 nm were clearly observed on the surface of GO sheets. At pH 5.0, irregular shaped nanoparticles were obtained and the average size of PB NPs gradually increased up to 58 nm, probably due to the slight hydrolysis of Fe^{3+}. In this study, irregular-shaped nanoparticles were easier to form at pH 3.0 as compared to other reports[20]. However, in our work there were also some cubic PB nanocrystals on the surface of GO at pH 5.0. A possible explanation could be the presence of carboxyl groups on the surface of GO which contributed to prevent the formation of $Fe(OH)_3$. The oxygen-containing functional groups are present on the surface of GO, as confirmed by FT-IR (Fig. 4), showing that the formation of cubic PB nanocrystals was dependent strongly on the pH value of the mixture. To fabricate high-quality PBNCs/GO nanocomposite, pH 1.6 was selected for growing PB nanocrystals on the GO nanosheets in this case.

It is well known that PB has been widely applied to chemically modified electrode[6, 10]. Herein we tried to immobilize PBNCs/GO composite onto the surface of Au electrode as an example to study a new possible application of the GO doped material in the third generation biosensor without any mediator. At pH 5.91 PBS, the two typical redox waves showed the oxidation of PB to Prussian green (PG). Reduction to Prussian white (PW) was also observed for the PBNCs/GO-modified Au electrode, indicating the effective presence of PB in the sample which could be applied in the field of electrochemistry. The potential separation of the pair of peaks (*ca*. 0.2 V) was only 39 mV, which is very close to the theoretical value, suggesting the fast charge transfer on the modified electrode. The effect of the potential scan rate on the peak current (i_{pa} and i_{pc}) at *ca*. 0.20 V (*i*) was investigated in the range of 5–1000 mV s^{-1} (Fig. 7). As expected, the peak currents increased linearly with the square root of scan rate ($v^{1/2}$), indicating that the observed electrochemical reaction was a diffusion-process.

The electrochemical stability of the PBNCs/GO/Au electrode was investigated with the cyclic voltammogram. The PBNCs/GO/Au electrode showed a good stability after scanned in PBS (pH 5.91) for 100 cycles. The peak currents decreased by 1.78%, indicating the monolayer film of PBNCs/GO was stable. However, the peak currents decreased by 78.75% after 100 cycles for PB/Au electrode. These results indicated that the presence of GO in the PBNCs/GO composite film greatly enhances the electrochemical stability of PB. The remarkable stability of the PBNCs/GO hybrid composite film could be due to the π-π stacking interaction between carbon atoms in the GO and the –CN groups of PB. Besides, cations in the PB (iron ions) might also be ready to interact with anions in the GO (carboxyl moieties) through ionic interaction and also, the hydrophobic interaction of the GO and PB might be contributed to the stability of the composite film [29,30].

The influence of PBS pH on the electrochemical behavior of PBNCs/GO-modified electrode was also studied. It has been reported that the PB layer was

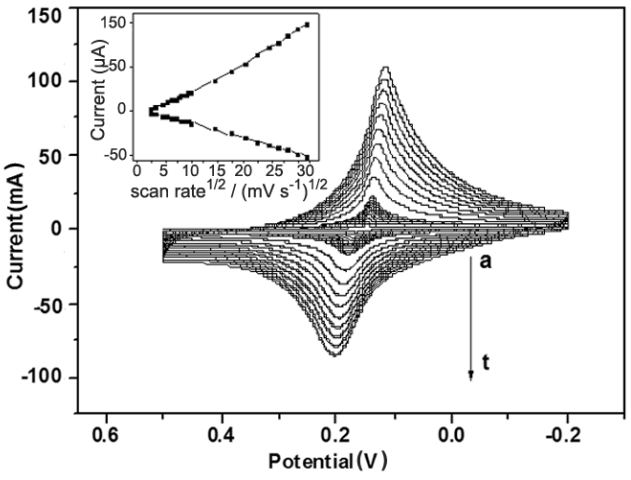

Fig. 7 — Cyclic voltammograms of PBNCs/GO composite modified Au electrode in PBS (pH 5.91) (containing 0.1 mol/L KCl) at various scan rates. [Curves a to t correspond to 5, 10, 20, 30, 40, 50, 60, 70, 80, 90, 100, 200, 300, 400, 500, 600, 700, 800, 900, 1000 mV s^{-1}. Inset: Plot of peak current at *ca*.0.2 V versus the square root of scan rate in the range of 5–1000 mV s^{-1}].

disrupted after a few scans at neutral pH and very low stability was observed with alkaline pH[31]. The reason was probably the strong interaction[32] between ferric ions (Fe^{3+}) and hydroxyl ions (OH^-) which forms $Fe(OH)_3$ at pH higher than 6.4, thus leading to the destruction of the Fe–CN–Fe bond[7]. For long this instability has been the main drawback in the use of PB modified electrodes. Pure PB modified electrode would lose about 54.39% of its efficiency when the pH rose from 4.5 to 6.0 and the redox currents would be lower at pH 7.0 and even disappear, indicating that pure PB film was unstable and dissolved. However, the PB NCs/GO hybrid film could improve the stability of PB at high pH. It was found that it always showed activity in neutral and weak alkaline solution. Moreover, it exhibited higher, well-defined and reversible redox peaks. This shows the potential application of such a film in biosensor fabrication because the optimum acidity for many enzymes was within the pH range of 6.5–8.0. It is assumed that the presence of carboxyl groups on the surface of GO contributes to prevent the formation of $Fe(OH)_3$.

In the potential range of 0.5 to −0.2 V, the cyclic voltammograms of the modified electrode in PBS before and after the addition of H_2O_2 were recorded. With the gradual addition of H_2O_2, the reduction peak current for PB increased while the oxidation peak current decreased gradually. More importantly, the reductive peak current of the CV curves of the fabricated PBNCs/GO/Au electrode was proportional to the concentration of H_2O_2. In the negative potential range, PB reduces to its reduction state PW, as shown in Eq. 1.

$$KFe(III)[Fe(II)(CN)_6] + e^- + K^+ \rightarrow K_2Fe(II)[Fe(II)(CN)_6] \quad \ldots (1)$$
(PB) (PW)

PW also exhibits catalytic activity for the reduction of H_2O_2 (Eq. 2).

$$2K_2Fe(II)[Fe(II)(CN)_6] + H_2O_2 \rightarrow 2KFe(III)[Fe(II)(CN)_6] + 2OH^- + 2K^+ \ldots (2)$$

Therefore, PB works as an electron-transfer mediator between the electrode and H_2O_2.

To determine the distribution of individual components, control experiments on GO/Au, PB/Au and PBNCs/GO/Au were carried out. With the addition of 1.5 mM H_2O_2, the reduction current increased, while the corresponding oxidation current decreased at all the electrodes. Obviously, both GO and PB are not good electrocatalyst for reducing H_2O_2 by themselves. However, once PBNCs/GO was modified on a gold electrode, the increase in cathodic current on PBNCs/GO/Au was >3 times larger than that on PB/Au and GO/Au. It can be seen that the current $I_{PBNCs/GO} > (I_{GO}+I_{PB})$, where $I_{PBNCs/GO}$ is the increased reduction current at the PBNCs/GO modified electrode after injection of 1.5 mM H_2O_2 and I_{GO} and I_{PB} are the increased reduction currents after injection of 1.5 mM H_2O_2 at GO and PB-modified gold electrodes, respectively. It is interesting that the amounts of PB in PB modified electrode and in PBNCs/GO modified electrodes are almost the same. Therefore, the increase of cathodic current on the PBNCs/GO composite film electrode is likely to be the result of synergism between GO and PBNCs.

In order to obtain good repeatability and high sensitivity an amperometric *i-t* curve was further tested. Figure 8 illustrates a typical current-time plot for PBNCs/GO/Au electrode on the successive addition H_2O_2 with the potential kept constant at –0.2 V. It can be seen that the amperometric signal is stable after the addition of H_2O_2 and the time required to attain 95% of the steady state response is less than 5 s. These data indicate that PBNCs/GO/Au electrode not only has high sensitivity, but also shows fast response to H_2O_2 with operating potential controlled at -0.2 V in 0.1 M PBS (pH 5.91). The calibration curve of H_2O_2 at PBNCs/GO/Au electrode is shown in upper inset of Fig. 8. The GO/PB/Au electrode exhibits a good linear relationship with H_2O_2 in the range of 0.002–2.8 mM with a correlation of 0.9985 and very low detection limit of 0.48 μM (S/N = 3). Thus,

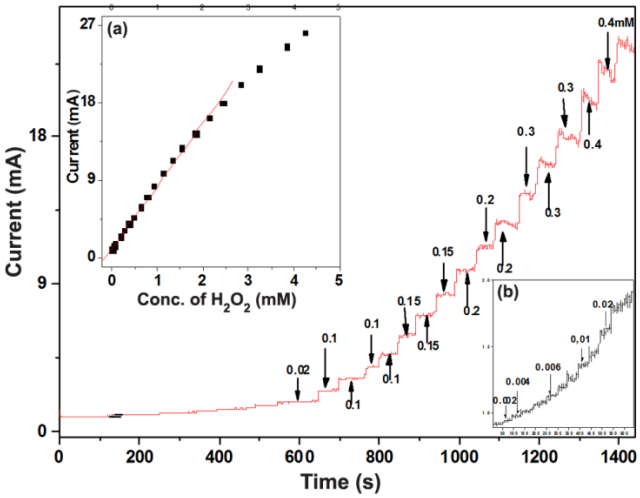

Fig. 8 — Amperometric response of PBNCs/GO/Au electrode to successive injection of H_2O_2 into 0.1 M PBS (pH 5.91) containing 0.1 M KCl. [Appl. potential −0.2 V. Inset (a): linear calibration curve; Inset (b): amplified response].

PBNCs/GO/Au electrode can be used to detect H_2O_2 as an amperometric sensor.

Conclusions

In summary, we have reported a novel and simple *in situ* synthetic route for the controlled preparation of PBNCs/GO heterogeneous composite materials. This synthetic route involves a mild heat-treatment process, which induces the *in situ* production of PB on GO surfaces. The heterogeneous nanostructures have been confirmed by SEM and TEM images. This route does not need the additional steps of reducing GO and introducing other reducing agents. More importantly, the coverage and loading of PB NPs on the surface of GO nanosheets can be tuned by control over the experimental parameters. In addition, this method is expected to be universal for preparing composites of GO and other coordination polymers.

Acknowledgement

This work was financially supported by the National Natural Science Foundation of China (21765015), the Open Funds of the State Key Laboratory of Electroanalytical Chemistry (SKLEAC201602) and the Jiangxi Province Food and Drug Administration Science Foundation (2016SP04), China.

References

1 Longchamp De & Hammond P, *Adv Funct Mater*, 14 (2004) 224.
2 Leventis N & Chung Y, *Chem Mater*, 4 (1992) 1415.
3 Itaya K, Ataka T & Toshima S, *J Am Chem* Soc, 104 (1982) 4767.
4 Torres G, Dupart E, Mingotaud C & Ravaine S, *J Phys Chem B*, 104 (2000) 9487.
5 Ding Y, Hu Y, Gu G & Xia X, *J Phys Chem C*, 113 (2009) 14838.
6 Karyakin A, Karyakina E & Gorton L, *Anal Chem*, 72 (2000) 1720.
7 Karyakin A & Karyakina E, *Sensors Actuators B*, 57 (1999) 268.
8 Li Z, Chen J, Li W, Chen K, Nie L & Yao S, *J Electroanal Chem*, 603 (2007) 59.
9 Qiu J, Xiong M, Liang R, Zhang J & Xia X, *J Nanosci Nanotechnol*, 8 (2008) 4453.
10 Qiu J, Peng H, Liang R, Li J & Xia X, *Langmuir*, 23 (2007) 2133.
11 GeimA & Novoselov K, *Nat Mater*, 6 (2007) 183.
12 Bunch J, Zande A, Verbridge S, Frank I, Tanenbaum D & Parpia J, *Science*, 315 (2007) 490.
13 Steurer P, Wissert R, Thomann R & Mülhaupt R, *Macromol Rapid Commun*, 30 (2009) 316.
14 Wang G, Wang B, Park J, Yang J, Shen X & Yao J, *Carbon*, 47 (2009) 68.
15 Hernandez Y, Nicolosi V, Lotya M M, Blighe F, Sun Z & De S, *Nat Nano*, 3 (2008) 563.
16 Goncalves G, Marques P, Granadeiro C, Nogueira H, Singh M & Grácio J, *Chem Mater*, 21 (2009) 4796.
17 Novoselov K, Geim A, Morozov S, Jiang D, Katsnelson M & Grigorieva I, *Nature*, 38 (2005) 197.
18 Wang P & Koberstein J, Macromolecules, 37 (2004) 5671.
19 Zhang Y, Sun X, Zhu L, Shen H & Jia N, *Electrochim Acta*, 56 (2011) 1239.
20 Cao L, Liu Y, Zhang B & Lu L, *ACS Appl Mater Interfaces*, 2 (2010) 2339.
21 Jiang Y, Zhang X, Shan C, Hua S, Zhang Q & Bai X, *Talanta*, 85 (2011) 76.
22 Liu X, Yao Z, Wang Y & Wei X, *Colloids Surf B*, 81 (2010) 508.
23 Hummers W & Offeman R, *J Am Chem Soc*, 80 (1958) 1339.
24 Choi H, Shim M, Bangsaruntip S & Dai H, *J Am Chem Soc*, 124 (2002) 9058.
25 Memming R, *Photoinduced Charge-Transfer Processes at Semiconductor Electrodes And Particles Electron Transfer I*, (Springer-Verlag, Berlin, Germany) 1994, pp. 105-181.
26 Vaucher S, M Li & Mann S, *Angew Chem In Ed*, 39 (2000) 1793.
27 Guo H, Wang X, Qian Q,Wang F & Xia X, *ACS Nano*, 3 (2009) 2653.
28 Shan C, Yang H, Han D, Zhang Q, Ivaska A & Niu L, *Langmuir*, 25 (2009) 12030.
29 Zhang J, Lee J, Wu Y & Murray R, *Nano Lett*, 3 (2003) 403.
30 Lin Y, Zhou B, Shiral Fernando K, Liu P, Allard L & Sun Y, *Macromolecules*, 36 (2003) 7199.
31 O'Halloran M, Pravda M & Guilbault G, *Talanta*, 55 (2001) 605.
32 Feldman B & Murray R, *Inorg Chem*, 26 (1987) 1702.